

RSC Advances



This is an *Accepted Manuscript*, which has been through the Royal Society of Chemistry peer review process and has been accepted for publication.

Accepted Manuscripts are published online shortly after acceptance, before technical editing, formatting and proof reading. Using this free service, authors can make their results available to the community, in citable form, before we publish the edited article. This *Accepted Manuscript* will be replaced by the edited, formatted and paginated article as soon as this is available.

You can find more information about *Accepted Manuscripts* in the [Information for Authors](#).

Please note that technical editing may introduce minor changes to the text and/or graphics, which may alter content. The journal's standard [Terms & Conditions](#) and the [Ethical guidelines](#) still apply. In no event shall the Royal Society of Chemistry be held responsible for any errors or omissions in this *Accepted Manuscript* or any consequences arising from the use of any information it contains.

Self-standing carbon nanotube forest electrodes for flexible supercapacitors**Jayesh Cherusseri^a and Kamal K. Kar^{a,b*}**

^aAdvanced Nanoengineering Materials Laboratory, Materials Science Programme, Indian Institute of Technology, Kanpur, Uttar Pradesh-208016, India.

^bAdvanced Nanoengineering Materials Laboratory Department of Mechanical Engineering, Indian Institute of Technology, Kanpur, Uttar Pradesh-208016, India.

*Corresponding author. Tel: +91-512-2597687, E-mail: kamalkk@iitk.ac.in (Kamal K. Kar)

Abstract

Self-standing, vertically aligned carbon nanotube forest grown on unidirectional carbon fibers have been fabricated by using chemical vapour deposition. The vertically aligned carbon nanotube forest grown on carbon fiber (VACNTF/UCF) was further used as electrode-current collector integrated system for fabricating a flexible supercapacitor. Highly bendable, electrically conductive unidirectional carbon fibers were used both as substrate for the growth of carbon nanotube forest and as current collectors for the supercapacitor. No other separate current collectors were used in this study. The Brunauer-Emmett-Teller surface area of VACNTF/UCF is found to be $553.8 \text{ m}^2 \text{ g}^{-1}$. The flexibility of VACNTF/UCF supercapacitor is tested by galvanostatic charge/discharge measurements by bending the supercapacitor at various angles. No significant variations in the supercapacitive properties were observed at different bending angles. Galvanostatic charge/discharge measurements show that the supercapacitor exhibits a volume specific capacitance of 3.4 F cm^{-3} with a high volume specific power density of 1195 mW cm^{-3} . The VACNTF/UCF supercapacitor also exhibits good cycling stability of more than 27000 cycles.

1. Introduction

Carbon nanotubes (CNTs) are one dimensional tubular materials of carbon and possess good electrical conductivity, large surface area, low density with high strength, chemical inertness, good electrochemical properties, etc. Hence these are effectively utilized in variety of applications such as electromechanical actuators,¹ field-effect transistors,² sensors,³ catalyst support materials for proton exchange membrane fuel cells,⁴ electrodes for supercapacitors,⁵ etc. CNTs based supercapacitive energy device is highly appreciated by the research community due to their exceptional performance. CNT supercapacitors possess high power densities, which enable quick delivery of energy within a fraction of second. The electrodes

for supercapacitors require properties such as large surface area, good electronic conductivity, and low mass density.⁶⁻⁸ As a result CNTs are the best candidates those can fulfil these requirements.

Among the various available methods of CNT production, chemical vapor deposition (CVD) is more suitable due to its simplicity.^{9,10} The preparation of CNT electrodes for supercapacitors include electrochemical deposition of CNTs on to electrically conducting substrates such as metal plates.^{11,12} These substrates are further used as secondary current collectors while assembling the supercapacitor device. But a major drawback of electrophoretic deposition method is that the procedure increases the contact resistance between the CNTs and substrate. An increased electrochemical series resistance is found to condemn the performance of the supercapacitor.¹³ Another drawback of using CNTs in an electrochemical deposition bath is the formation of aggregates in the form of CNT bundles by joining tens to hundreds of nanotubes together. CNTs may be joined in parallel and entangled manner in order to form a hair-ball like structure with a reduction in its specific surface area. This results in decaying the electrochemical properties as the CNT electrode/electrolyte interaction diminishes due to its lower surface area. A best solution to these problems is avoiding the electrochemical deposition used for manufacturing the CNT electrodes and synthesizing CNTs directly on carbon substrates by CVD. By this way, CNTs grown on carbon substrates help in reducing the electrochemical series resistance and also avoid the electrochemical deposition for manufacturing the CNT electrodes for supercapacitors. Agnihotri et al. have used carbon fibers as substrate for the growth of entangled CNTs with less density¹⁴ but they couldn't achieve vertically aligned growth of CNTs on carbon fibers. These entangled CNTs can't function as electrode materials due to their lower surface area and reduced electrochemical properties. Particularly for supercapacitor electrodes, vertically aligned CNTs are indeed since only vertically aligned CNTs possess large specific surface

area. In the recent past, flexible supercapacitors have achieved much popularity as these can be easily incorporated in to flexible electronic devices. Among the other electrode materials, CNTs¹⁵ and its nanocomposites¹⁶ have been potentially used for preparing highly flexible supercapacitors with solid state polymer electrolytes.

In this study, we report the synthesis of self-standing, vertically aligned CNT forest (VACNTF) grown on unidirectional carbon fibers (UCFs) with high density and it functions as electrode-cum-current collector for flexible supercapacitor. By synthesizing VACNTF on flexible and electrically conducting UCFs, one can decrease the contact resistance of electrode/current collector interface as well as can avoid the use of secondary current collectors. To the best of our knowledge, the use of VACNTF grown on UCF (VACNTF/UCF) as electrode-cum-current collector in flexible supercapacitors is not yet reported. Here, no separate current collectors are used whereas the uncoated portion of UCFs were used as current collectors for fabricating the supercapacitor device. The electrode-cum current collector integrated system helps in reducing the mass of supercapacitor as compared to that of supercapacitors utilizing metallic current collectors.

2. Experimental methods

2.1 Materials

Polyacrylonitrile based UCFs (specific density ~ 1.8 g/cc, tensile strength ~ 1900 - 2750 MPa, diameter ~ 6 - 7 μm) were received from M/S Fortafil Industries Inc., U.K. Nickel sulphate hexahydrate ($\text{NiSO}_4 \cdot 6\text{H}_2\text{O}$, 99%), ammonium chloride (NH_4Cl , 99%), tri-sodium citrate ($\text{Na}_3\text{C}_6\text{H}_5\text{O}_7 \cdot 2\text{H}_2\text{O}$, 98%), liquor ammonia (NH_3 , 25%) were obtained from M/S Qualigens Fine Chemicals, India. Sodium hypophosphite ($\text{NaH}_2\text{PO}_2 \cdot \text{H}_2\text{O}$, 99%) and potassium hydroxide (KOH , 99%) were obtained from M/S Loba Chemie Pvt. Ltd., India.

2.2 Synthesis of CNT forest on carbon fibers

UCFs having individual fiber diameter of $\sim 8 \mu\text{m}$, were used as substrate to grow VACNTF by CVD. To grow VACNTF on CF, the as-received UCFs were firstly heated in air at $400 \text{ }^\circ\text{C}$ for 10 min followed by washing with acetone to remove the polymer sizing agent. An electroless coating method was used to deposit nickel catalyst on the surface of UCFs.¹⁷ The various chemicals used in the electroless coating bath, their concentrations and functions are summarized in Table S1. The UCF strands were dipped in the coating bath kept at $85 \text{ }^\circ\text{C}$ under constant magnetic stirring for a deposition time of 10 min, rinsed severally with propanol and deionized water and dried at $85 \text{ }^\circ\text{C}$ for 24 h. Further, VACNTF was synthesized on UCFs by CVD using acetylene as carbon precursor. In this process, the nickel coated UCFs were heated to $500 \text{ }^\circ\text{C}$ in a horizontal quartz furnace (1.12 m length with 105 mm diameter) under a continuous N_2 flow (200 ml min^{-1}). In order to reduce the formation of oxides on the nickel particles, H_2 was introduced at a flow rate of 100 ml min^{-1} for 15 min. The temperature was further increased to $700 \text{ }^\circ\text{C}$ and acetylene was introduced at a flow rate of 90 ml min^{-1} for 15 min while keeping the N_2 flow fixed at 200 ml min^{-1} throughout. The VACNTF samples were collected after cooling down the furnace to room temperature under N_2 flow.

2.3 Assembly of supercapacitor cell

A symmetric supercapacitor device was fabricated with VACNTF grown on UCFs as electrode-cum-current collector integrated system, without any further modification. The dimension of supercapacitor cell was 30 mm (length), 1.5 mm (width), and 0.22 mm (thickness). Two similar pieces of VACNTF/UCF strands were kept parallel on both sides of an electrolyte-filled filter paper and kept in between two highly flexible teflon sheets (with thickness of 0.4 mm) (Fig. S1). The uncoated portion of VACNTF/UCF was utilized as current collecting lead and no separate current collectors were used in this study. Fig. 1

provides the schematic of overall process involving in the fabrication of flexible supercapacitor with VACNTF/UCF electrode-cum-current collector integrated system.

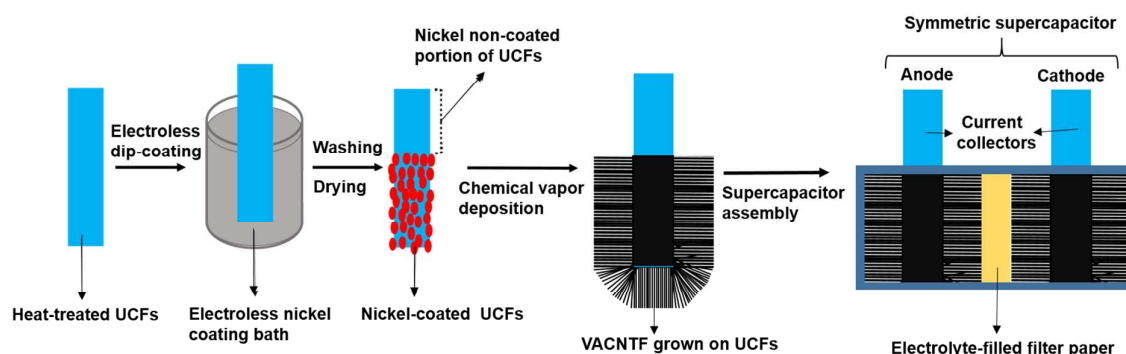


Fig. 1. Schematic illustrating the overall process of fabricating flexible supercapacitor with VACNTF/UCF electrode-cum-current collector integrated system.

2.4 Materials Characterizations

The microstructure and surface topography of the VACNTF/UCF electrodes were studied using a scanning electron microscope (SEM Carl Zeiss EVO MA 15). Energy dispersive X-ray analysis was carried out by EDAX spectrometer (EDS; INCA Penta FETx3, Oxford Instruments, UK), attached to SEM (Carl Zeiss, EVO50, Oberkochen, Germany) to know the elemental composition of nickel coated UCFs. An X-ray diffractometer was used to characterize the crystalline structure of the electrodes. The X-ray diffraction (XRD) patterns of the samples were obtained using a Cu K radiation system (Rigaku MiniFlex 600). The thickness of electrodes and the supercapacitor device were measured by using a thickness gauge (S. C. Dey & Co., India). Raman spectra of the CNT forest samples were analyzed with the help of LabRam Micro Raman Spectrometer (Jobin-Yuon HR 800 UV) by using a He-Ne (632.7 nm) laser excitation source. The N₂ sorption surface area measurement of VACNTF/UCF was performed with a surface area analyzer (Quantachrome Autosorb I-C, U.S.A). The mass of CNTs was measured by using a microbalance with readability of 1 µg (XP 6, Mettler Toledo).

2.5 Supercapacitor device testing

A two-electrode cell configuration was used to measure the performance of the as-fabricated supercapacitor. The supercapacitor was assembled using two pieces of VACNTF/UCF as electrode-cum-current collector, and a piece of filter paper soaked with 5 M KOH aqueous electrolyte was used as a separator. Cyclic voltammetry (CV), electrochemical impedance spectroscopy, and galvanostatic charge/discharge were used to investigate the electrochemical performance of the supercapacitor cell. Every electrochemical test was carried out by using CHI 608D instrument (CHI Instruments, U.S.A.). CV measurement was carried out in between -0.6 to 0.6 V at different scan rates. All the calculations related to the supercapacitor cell testing are discussed in the electronic supplementary information.

3. Results and discussion

The surface topography of the catalyst coated UCFs is presented in Fig. 2a. The nickel nanoparticles are coated uniformly over the surface of UCFs and serve as catalyst supports for the growth of VACNTF. Figs. 2b-d represent the SEM images of highly dense VACNTF grown on nickel coated UCFs by CVD. The average diameter of VACNTF lie in between 50 to 150 nm and few millimeters in length. The achievement of vertical growth on CNTs with high density is attributed to the electroless coating bath concentration and also the pH of the bath. The uncoated portion of UCFs does not support the growth of VACNTF and hence it is used as current collector for the supercapacitor. The novel VACNTF/UCF architecture as electrode-cum-current collector for fabricating the supercapacitor cell is not reported yet. The VACNTF/UCF integrated system is beneficial to the supercapacitors in terms of low cost of preparation, simple processing method, light-weight, and superior electrochemical performance. The three dimensional structure is found helpful in improving the capacitance

and ionic conductivity of the supercapacitor cell by triggering the ion diffusion across its pores and will be discussed later.

The XRD patterns of UCFs and nickel coated UCFs are depicted in Fig. S2. For both the spectra, the diffraction peak at 25.5° can be assigned to the C (200) plane of graphitic carbon (JCPDS file no.41-1487). For the spectra of nickel coated UCFs, the two major peaks at 44.5° and 52.2° can be assigned to the (111) and (200) planes of nickel (JCPDS file no.88-2326). The effect of electroless deposition time on the properties of nickel coating on UCFs was studied by EDAX. The EDAX spectra shown in Fig. S3 indicates that the amount of nickel coated on UCFs is 11.9 wt %. These nickel particles are helpful in the growth of VACNTF on UCFs.

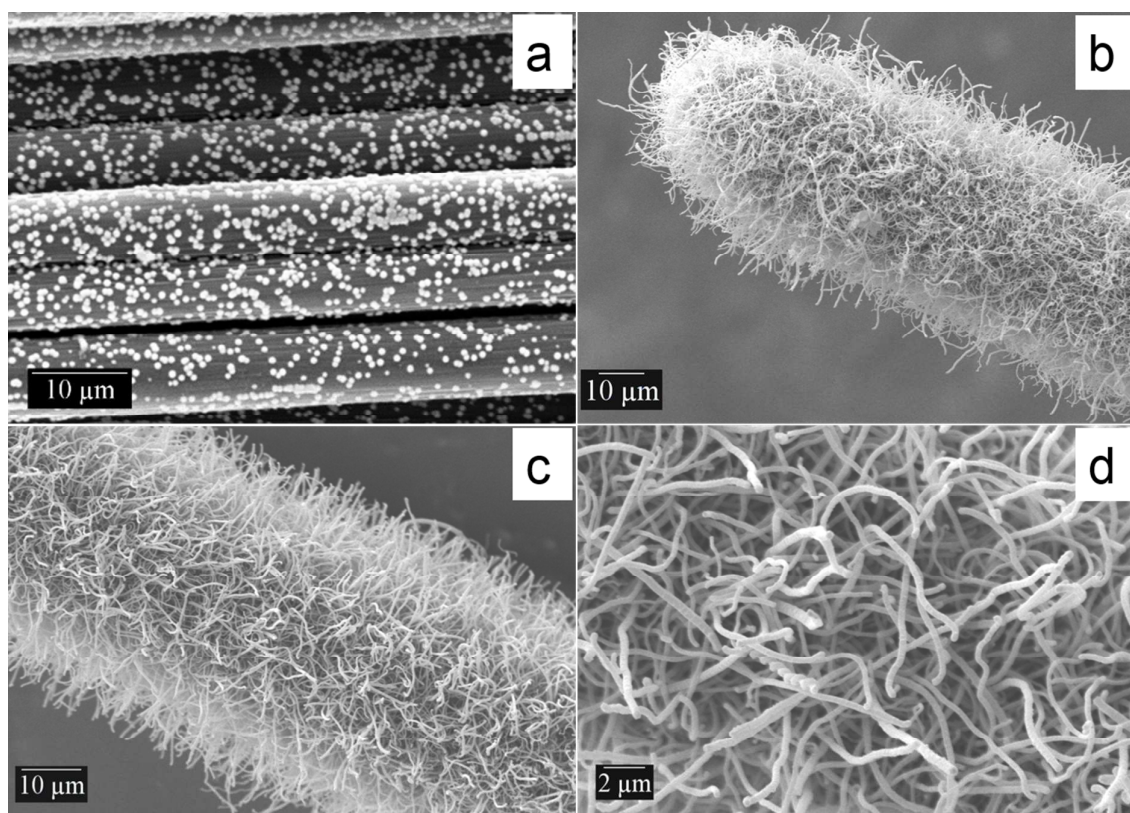


Fig. 2. SEM images of nickel-coated UCFs (a), VACNTF grown on UCFs at different magnifications (b-d).

Raman spectra of VACNTF/UCF depicted in Fig. 3 contain two major peaks at 1330 and 1590 cm^{-1} can be assigned to D-band and G-band of CNTs, respectively. The D-band represents defects and lattice distortions in carbon structures¹⁸ whereas the G-band is associated with stretching vibration of graphite crystals¹⁹. The I_D/I_G ratio of VACNTF/UCF is 0.87 and this value indicated that the as synthesized CNTs are having good electronic conductivity.

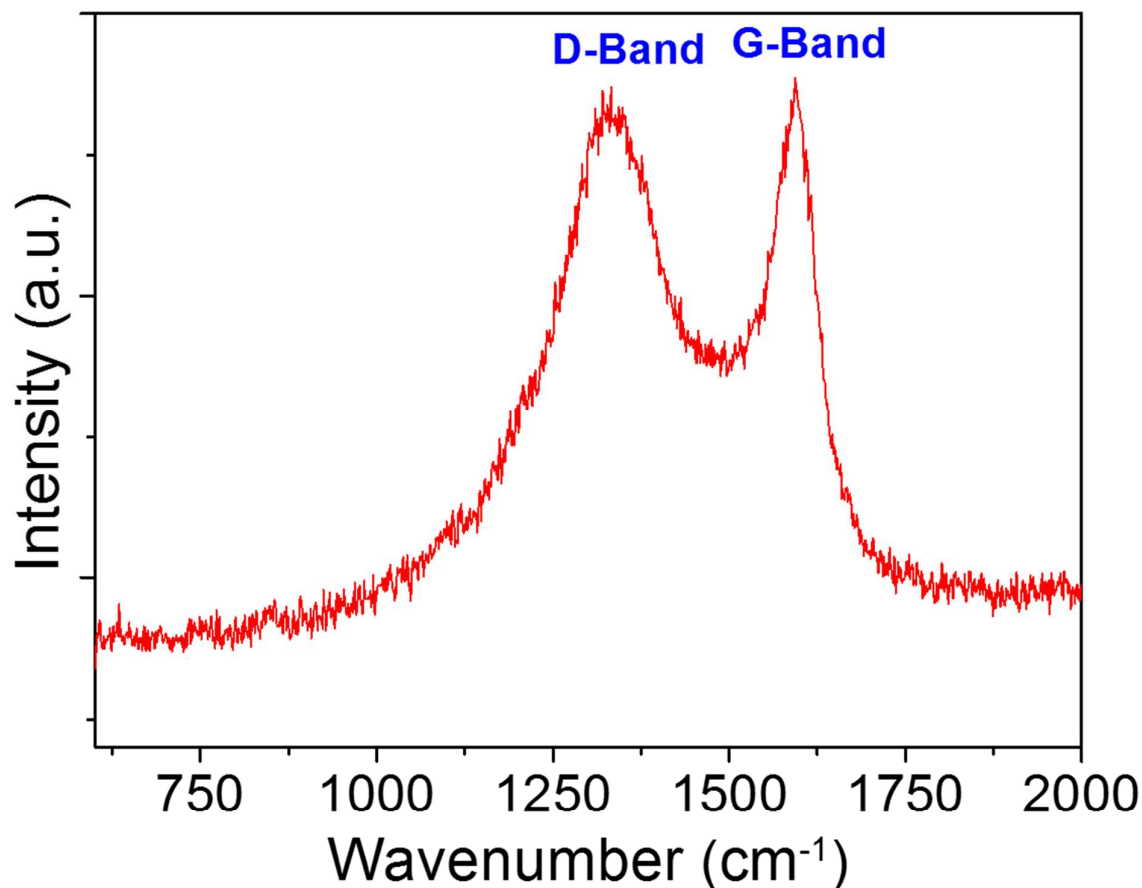


Fig. 3. Fingerprint Raman spectra of CNT forest grown on carbon fibers.

The N_2 sorption surface area of VACNTF/UCF is calculated by Brunauer-Emmett-Teller (BET) method. The sorption isotherms shown in Fig. 4a indicate that the nature of adsorption process is type-V in nature, which shows the capillary condensation of gas within

the porous architecture of VACNTF/UCF. The BET surface area of VACNTF/UCF is $553.8 \text{ m}^2 \text{ g}^{-1}$. This large value indicates that the VACNTF are not formed an entangled structure or hair-ball, can easily be verified from SEM (Figs. 2b-d). The open pore structure is effectively utilized by the gas molecules during the N_2 sorption process. The total pore volume of VACNTF/UCF is $1.121 \text{ cm}^3 \text{ g}^{-1}$ for pores smaller than 3258.5 \AA (diameter) at $P/P_0 = 0.99$. The average pore diameter of VACNTF/UCF is 8 nm , calculated from Barrett-Joyner-Halenda (BJH) pore-size distribution curve (Fig. 4b). From the BJH curve, it is clear that the specific surface area of VACNTF/UCF is mainly contributed by the three dimensional mesopores.

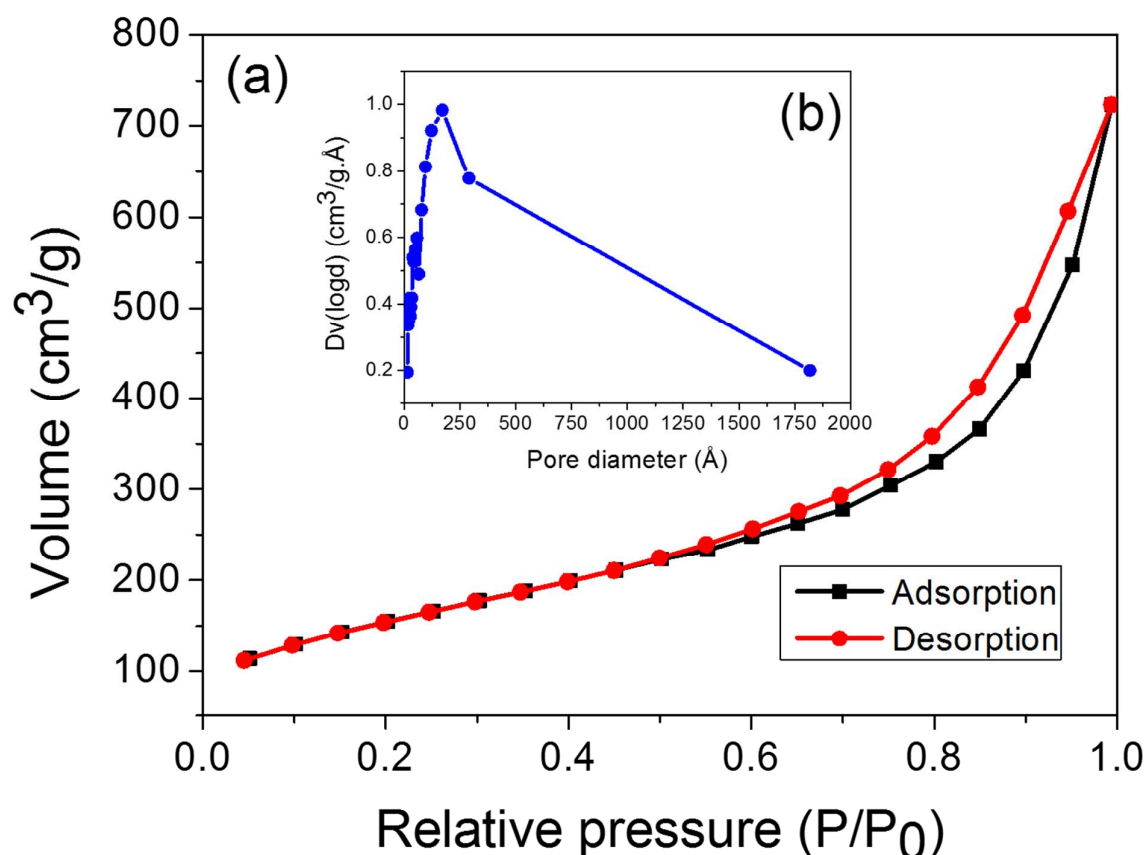


Fig. 4. (a) N_2 sorption isotherms of CNT forest grown on carbon fibers and (b) BJH pore-size distribution curve.

From all the above analyses, self-standing VACNTF/UCF electrode-cum-current collectors are beneficial to use in supercapacitors since it possess large surface area, mesoporous structure, light-weight, etc. These parameters are the pre-requisites for electrodes in supercapacitors and hence they can achieve high specific capacitances along with high power densities.^{20,21} Apart from these parameters, the VACNTYF/UCF is highly bendable and hence suitable for the fabrication of flexible supercapacitors.

The electrochemical impedance spectra, represented by Nyquist plot of VACNTF/UCF supercapacitor cell is shown in Fig. 5a and the high frequency impedance plot is given as an inset. From Fig. 5a, it is clear that VACNTF/UCF supercapacitor exhibits a low bulk electrolyte resistance ($R_b \sim 1.8 \Omega$). A lower value of R_b indicates high ionic conductivity possess by the VACNTF/UCF electrode-cum-current collectors and this may be due to the same graphitic carbon components within the integrated system (CNTs and UCFs). The ionic conductivity of the CNT forest supercapacitor electrodes is $8.8 \times 10^{-2} \text{ S cm}^{-1}$, indicates that the electrodes enhance the ion diffusion through its mesopores during the rapid charging/discharging. The reason behind this high ionic conductivity may be attributed to the robust conductive paths available on the free standing electrode-cum-current collectors.

The CV curves VACNTF/UCF supercapacitor cell at different scan rates are depicted in Fig. 5b. The CV curves represent a typical $I - E$ characteristics of CNT electrodes. The near-ideal rectangular CV curves (as no redox peaks are observed) are clear evidence of the double layer charge storage possess by CNTs. Flexible supercapacitors have achieved great demand in wearable electronics. In order to examine the flexibility of the present supercapacitor cell, the electrochemical characterizations have been carried out by bending the supercapacitor cell at various angles. The various angles selected for bending the supercapacitor are 150, 90, 45, 20, and 0° and the way by which the angles are selected is

shown in Fig. S4. The galvanostatic charge/discharge measurement of the supercapacitor cell is carried out at different current densities such as 2.2, 5.5, and 11.1 mA cm⁻² and is shown in Fig. 5c. From Fig. 5c, it can be seen that the supercapacitor cell can be charged with a high current density of 11.1 mA cm⁻², without affecting the charge/discharge profiles. The galvanostatic charge/discharge measurement is extended for various supercapacitor bending angles at a current density of 11.1 mA cm⁻² and the corresponding charge/discharge curves are shown in Fig. 5d. The symmetric galvanostatic charge/discharge curves represent the ideal capacitive behaviour of VACNTF/UCF supercapacitor. From Fig. 5d, it is clear that there is no significant variation in the charging/discharging behaviour while bending from its straight position (i.e., 180 °) towards 0 °. A similar behaviour is observed in the VACNTF/UCF supercapacitor from the CV study carried out in between 0 and 0.6 V at 300 mV s⁻¹ and at various supercapacitor bending angles (Fig. S5). The nature of CV curves was unaltered during the supercapacitor bending. No significant variation is observed in both the galvanostatic charge/discharge and CV curves even at a bending angle of 0 °, indicates high bendability of the VACNTF/UCF supercapacitor cell.

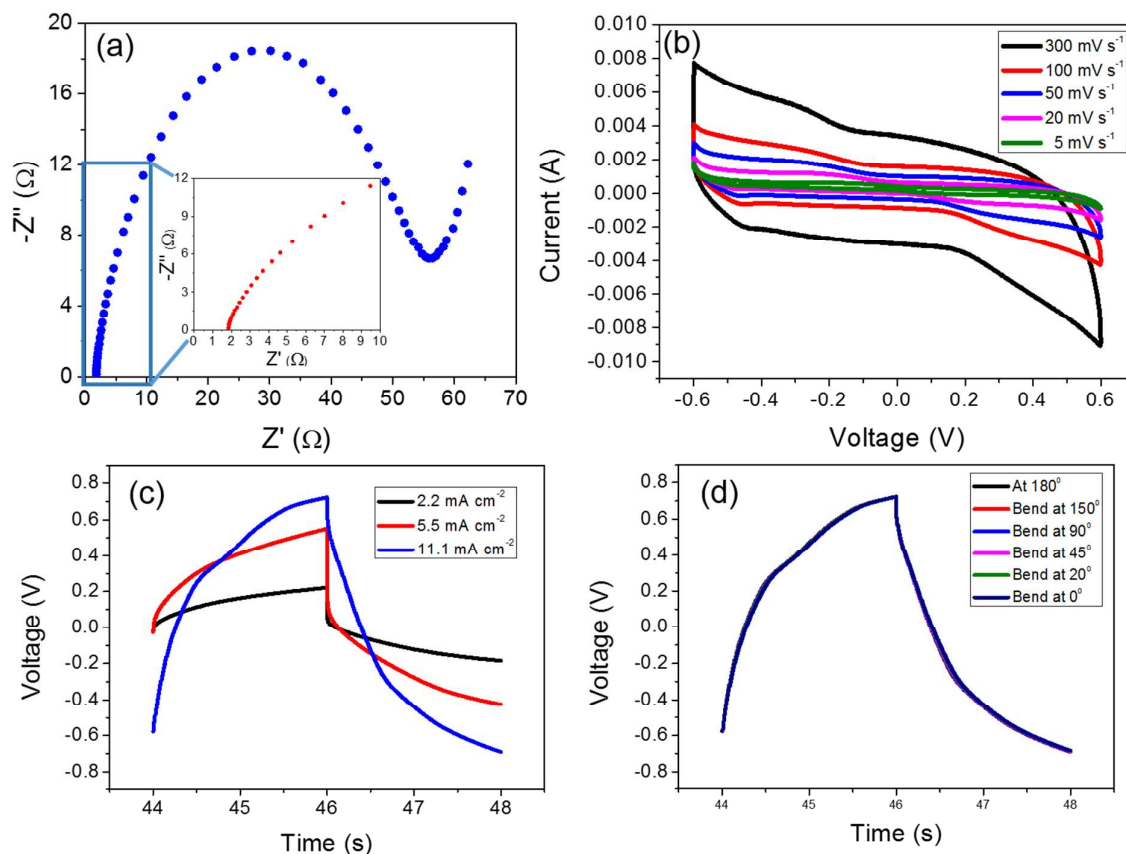


Fig. 5. (a) Nyquist plot (Inset: enlarged portion in the high frequency region), (b) CV curves at various scan rates, (c) galvanostatic charge/discharge curves at different current densities, and (d) galvanostatic charge/discharge curves at various bending angles for the VACNTF/UCF supercapacitor.

The supercapacitor cell exhibits a volume specific capacitance of 3.4 F cm^{-3} , this high value is attributed to the large specific surface area and the mesoporous structure of VACNTF electrodes. Self-standing VACNTF electrodes possess a unique three dimensional open mesoporous structure, which facilitates faster ion diffusion and an enhanced charge storage is achieved. As the pore size is distributed around 8 nm, mesoporous VACNTF electrodes undergone faster charging/discharging with high reversibility. This enhanced performance can't be achieved if the CNTs were not grown vertically on the surface of UCFs. Hence the method of preparing novel electrode-cum-current collector integrated system by

using VACNTF/UCF is mainly responsible for the superior performance of the supercapacitor cell. The volume specific capacitance reported for the VACNTF/UCF supercapacitor is the highest among the CFs based supercapacitors reported earlier.^{22,23} No significant change in the specific capacitance is observed while bending the supercapacitor towards smaller angles. The specific capacitance variation with respect to bending angle is shown in Fig. 6a, it is clear that there is no significant reduction even at 0° bending state. This shows that the supercapacitor can bend at any angle without deteriorating its electrochemical properties. The CNT forest supercapacitor also exhibits a mass specific capacitance of 103 F g⁻¹ and this value is comparatively higher for the supercapacitor manufactured with pristine CNTs based electrodes. Table S2 compares the electrochemical performance of CNT forest supercapacitor with other CNTs based supercapacitors. The mass specific capacitance is found to be unaltered at supercapacitor bending angles and is shown in Fig. S6. The supercapacitor exhibits a high volume specific energy density of 0.664 mWh cm⁻³ with a corresponding volume specific power density of 1195 mW cm⁻³ as shown in Figs. 6b and 6c, respectively. The power density exhibited by VACNTF/UCF supercapacitor is the highest among the UCFs based supercapacitors reported such as MnO₂/CF supercapacitor,²² co-axial fiber supercapacitor,²³ and ZnO core/shell supercapacitor.²⁴ The electrochemical performance of VACNTF/UCF supercapacitor is unaffected even at a maximum bending angle of 0°, which shows its ultra-high bendability and such a highly bendable supercapacitor is not reported so far.^{22, 25-27} Ragone plot for VACNTF/UCF supercapacitor is shown in Fig. 6d.

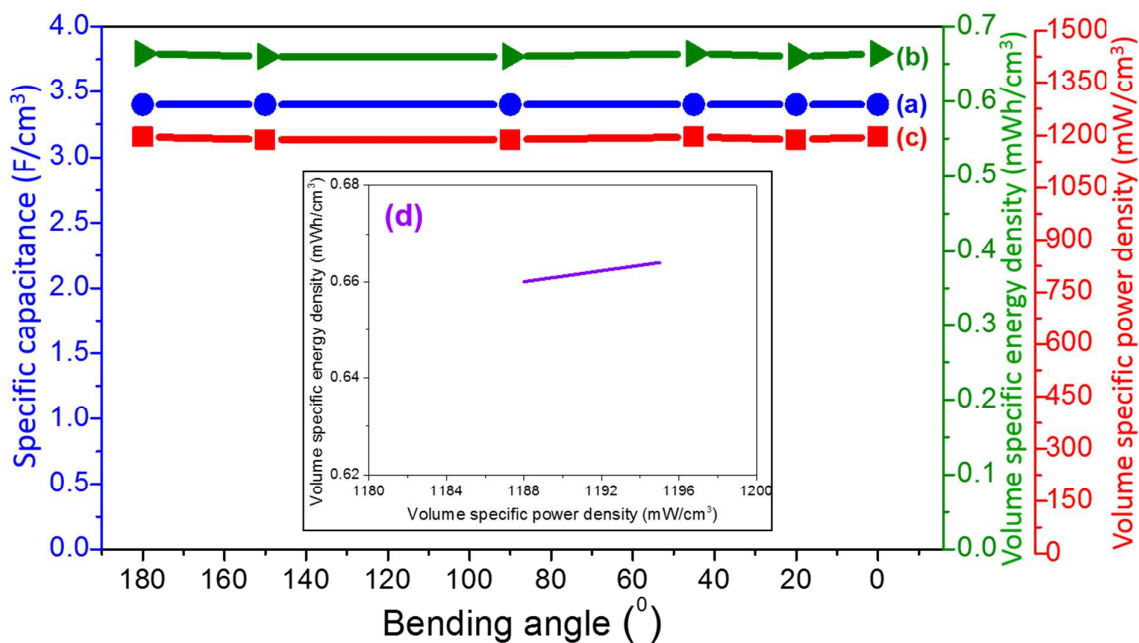


Fig. 6. Plots of variations in specific capacitance (a), volume specific energy density (b), and volume specific power density (c) with respect to supercapacitor bending angle; Ragone plot for VACNTF/UCF supercapacitor (d).

The VACNTF/UCF supercapacitor exhibits a volumetric capacitance of 586 mF cm^{-3} . The variation in volumetric capacitance at various bending angles is shown in Fig. 7a. From Fig. 7a, it is clear that there is no significant change even at a bending angle of 0° . The volumetric capacitance retention with respect to bending angles are shown in Fig. S7. The supercapacitor cell exhibits a volumetric energy density of $0.114 \text{ mWh cm}^{-3}$ with a corresponding volumetric power density of 205 mW cm^{-3} are shown in Figs. 7b and 7c, respectively. The percentage variation in the volumetric energy and power densities for the VACNTF/UCF supercapacitor cell with respect to bending angles are depicted in Fig. S8. The digital image of VACNTF/UCF supercapacitor cell bend at 90° is shown in Fig. 7d, which indicates the ultra-high bendability of VACNTF/UCF supercapacitor.

From all the above results, it can be say that the VACNTF/UCF supercapacitor can bend at any angle without sacrificing its charge/discharge behaviour. Hence the

supercapacitor utilizing novel VACNTF/UCF electrode-cum-current collector integrated system is a promising candidate for flexible, high power supercapacitors.

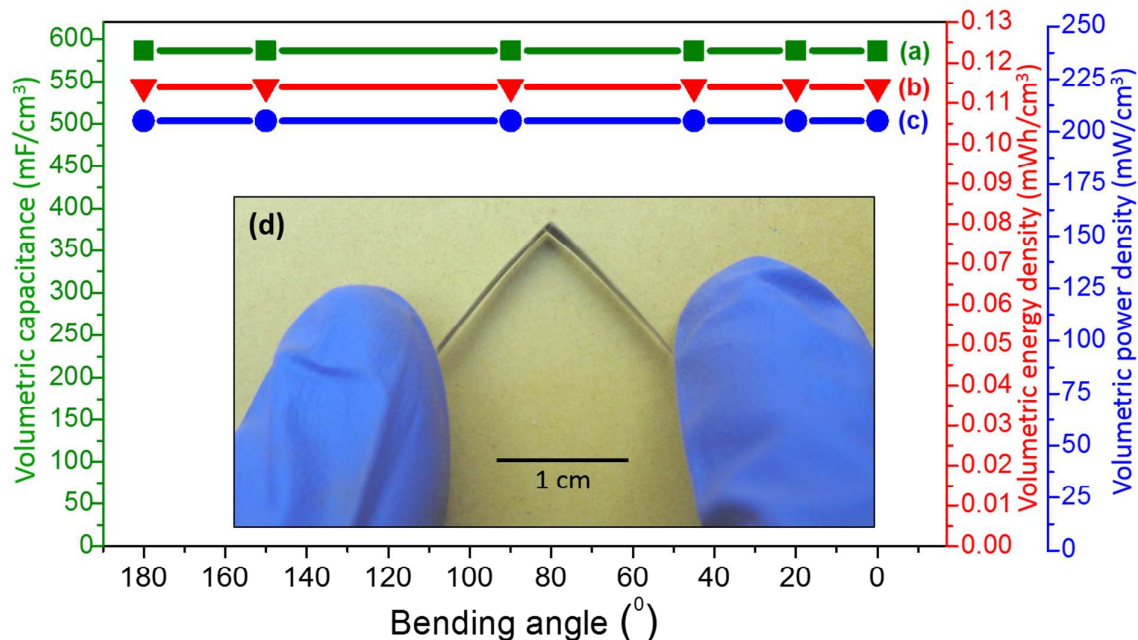


Fig. 7. Plots of variations in volumetric capacitance (a), volumetric energy density (b), and volumetric power density (c) with respect to supercapacitor bending angle; Digital image of VACNTF/UCF supercapacitor bend at 90° (d).

For practical applications, cycle life of the supercapacitor is very important. In order to estimate the cycle life of VACNTF/UCF supercapacitor, galvanostatic charge/discharge study has been carried out for 27000 charge/discharge cycles at a current density of 11.1 mA cm⁻² at a supercapacitor bending angle of 90°. The volume specific capacitance of VACNTF/UCF supercapacitor at various charge/discharge cycle numbers is shown in Fig. 8a. An increase in the volume specific capacitance can be seen at its 8000 cycle (3.5 F cm⁻³), the reason for this increased capacitance may be due to the stabilization process of the supercapacitor after certain number of cycles. In the initial stages of charge/discharge

cycling, more number of pores might have open within the VACNTF three dimensional network, which has triggered faster diffusion of ions and hence the capacitance is slightly increased. But soon after 8000 cycles, the specific capacitance is decreased gradually and an almost stable performance can be observed from 12000 cycles till the end of 27000 cycle. The percentage retention of specific capacitance with respect to cycle numbers is given in Fig. S9. Highly flexible VACNTF/UCF supercapacitor exhibits a high specific capacitance of 2 F cm^{-3} even after 27000 cycles, which shows its good cycling stability. Hence VACNTF/UCF supercapacitor has proved its long cycle life by functioning for 27000 cycles along with superior electrochemical performance. From this study, we can say that no other CNT/fibrous carbon based supercapacitors reported so far²²⁻²⁷ has achieved a stable performance with high capacitance, as compared to the present supercapacitor.

Similar variations can be viewed in the case of areal (Fig. S10) and volumetric capacitance (Fig. 8b) also. The VACNTF/UCF supercapacitor exhibits a volumetric capacitance of 348 mF cm^{-3} at 27000 cycle. The galvanostatic charge/discharge curves of the supercapacitor just before the completing its 27000 cycles is shown in Fig. 8c. From Fig. 8c, it is clear that the curves are highly symmetrical with charge/discharge counterparts and exhibit good linear voltage-time profiles. From the galvanostatic charge/discharge cycling test, it can be say that the performance of VACNTF/UCF supercapacitor is much better than the presently available flexible high power supercapacitors in terms of high specific capacitance, ultra-high power density, long cycle life, easy processability, and low cost.

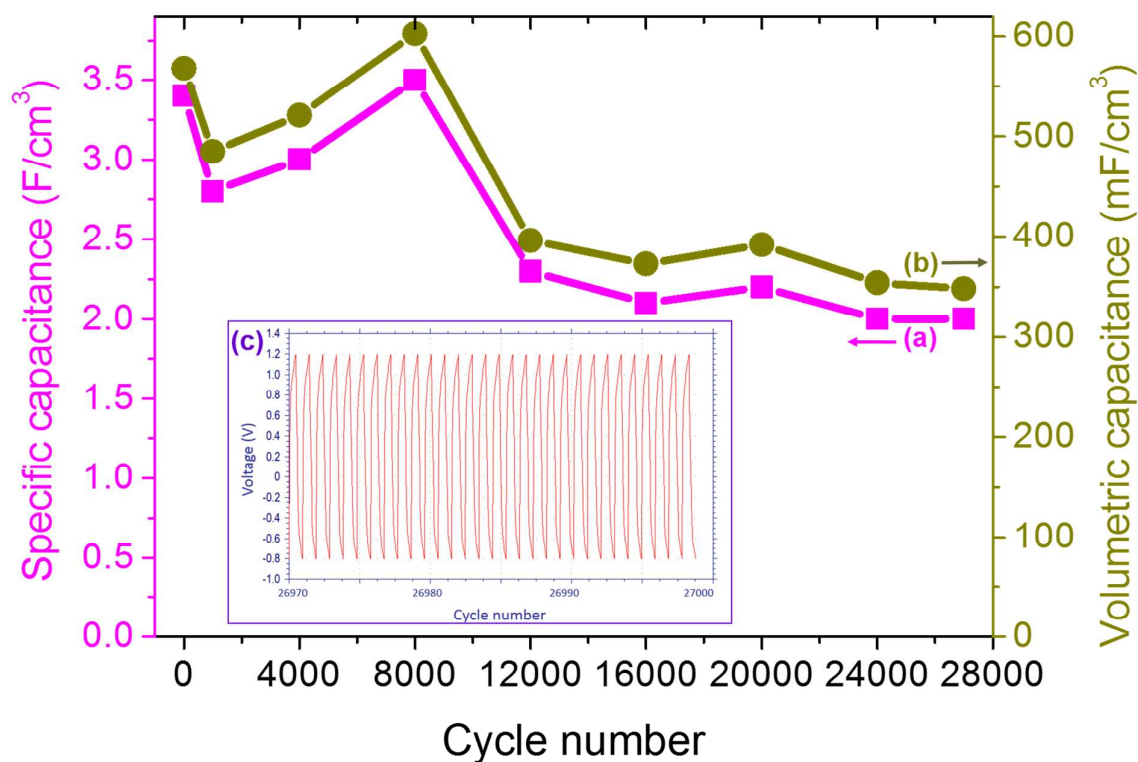


Fig. 8. Plots of variations in specific capacitance (a) and volumetric capacitance (b) with respect to galvanostatic charge-discharge cycle number; (c) galvanostatic charge/discharge curves of VACNTF/UCF supercapacitor just before completing 27000 cycles.

4. Conclusions

A highly flexible supercapacitor has been fabricated with highly bendable self-standing VACNTF/UCF electrode-cum-current collector integrated system. Uncoated portion of UCFs were functioned as current collector for the supercapacitor and no separate secondary current collectors were used. The supercapacitor experiences a low electrochemical series resistance, which has triggered the rapid ion diffusion processes during its operation. The flexibility of VACNTF/UCF supercapacitor has been tested by CV and galvanostatic charge/discharge measurements by bending the supercapacitor at different angles and which shows no significant changes both in the CV and galvanostatic charge/discharge curves even at a supercapacitor bending at 0°. Highly flexible VACNTF/UCF supercapacitor exhibits a high

volume specific capacitance of 3.4 F cm^{-3} with a high volumetric power density of 1195 mW cm^{-3} along with a cycle life of more than 27000 cycles. The present study proclaims the development of novel VACNTF/UCF electrode-cum-current collector integrated system for flexible supercapacitors, which can be used in other energy conversion and storage devices also.

Acknowledgement:

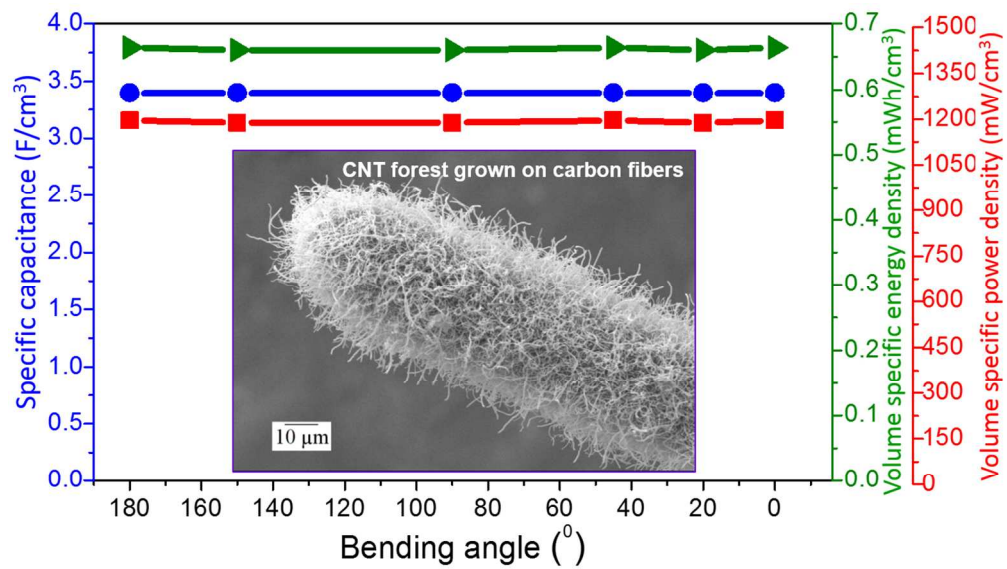
This work was supported by the Indian Institute of Technology Kanpur, India. The authors acknowledge Dr. Malay K. Das, Department of Mechanical Engineering, Indian Institute of Technology Kanpur, India for providing the experimental facility for this work.

References

1. L. Lu and W. Chen, *Nanoscale*, 2011, 3, 2412-2420.
2. J-H. Jin, J. Kim, T. Jeon, S-K. Shin, J-R. Sohn, H. Yi, and B. Y. Lee, *RSC Adv.*, 2015, 5, 15728-15735.
3. G. P. Evans, D. J. Buckley, N. T. Skipper, and I. P. Parkin, *RSC Adv.*, 2014, 4, 51395-51403.
4. W. Yuan, S. Lu, Y. Xiang, and S. P. Jiang, *RSC Adv.*, 2014, 4, 46265-46284.
5. X. Li, W. Sun, L. Wang, Y. Qi, T. Guo, X. Zhao, and X. Yan, *RSC Adv.*, 2015, 5, 7976-7985.
6. C. Du and N. Pan, *J. Power Sources*, 2006, 160, 1487-1494.
7. J. H. Chen, W. Z. Li, D. Z. Wang, S. X. Yang, J. G. Wen, and Z. F. Ren, *Carbon*, 2002, 40, 1193-1197.
8. A. G. Pandolfo and A. F. Hollenkamp, *J. Power Sources*, 2006, 157, 11-27.
9. J-H. Lin, Z-Y. Zeng, Y-T. Lai, and C-S. Chen, *RSC Adv.*, 2013, 3, 1808-1817.

10. A. Gohier, C. P. Ewels, T. M. Minea, and M. A. Djouadi, *Carbon*, 2008, 46, 1331-1338.
11. Z. Yu, L. Tetard, L. Zhai, and J. Thomas, *Energy Environ. Sci.*, 2015, 8, 702-730.
12. A. R. Boccaccini, J. Cho, J. A. Roether, B. J. C. Thomas, E. J. Minay, and M. S. P. Shaffer, *Carbon*, 2006, 44, 3149-3160.
13. P. Liu, M. Verbrugge, and S. Soukiazian, *J. Power Sources*, 2006, 156, 712-718.
14. P. Agnihotri, S. Basu, and K. K. Kar, *Carbon*, 2011, 49, 3098-3106.
15. Z. Niu, H. Dong, B. Zhu, J. Li, H. H. Hng, W. Zhou, X. Chen, and S. Xie, *Adv. Mater.*, 2013, 25, 1058-1064.
16. C. Meng, C. Liu, L. Chen, C. Hu, and S. Fan, *Nano Lett.*, 2010, 10, 4025-4031.
17. K. K. Kar and D. Sathiyamoorthy, *J. Mater. Process. Technol.*, 2009, 209, 3022-3029.
18. F. Tuinstra and J. L. Koenig, *J. Chem. Phys.*, 1970, 53, 1126-1130.
19. A. Kasuya, Y. Sasaki, Y. Saito, Y. Kohji, and Y. Nishina, *Phys. Rev. Lett.*, 1997, 78, 4434-4437.
20. S. T. Mayer, R. W. Pekala, and J. L. Kaschmitter, *J. Electrochem. Soc.*, 1993, 140, 446-451.
21. I. Tanahashi, A. Yoshida, and A. Nishino, *J. Electrochem. Soc.*, 1990, 137, 3052-3057.
22. X. Xiao, T. Li, P. Yang, Y. Gao, H. Jin, W. Ni, W. Zhan, X. Zhang, Y. Cao, J. Zhong, L. Gong, W-C. Yen, W. Mai, J. Chen, K. Huo, Y-L. Chueh, Z. L. Wang, and J. Zhou, *ACS Nano*, 2012, 6, 9200-9206.
23. V. T. Le, H. Kim, A. Ghosh, J. Kim, J. Chang, Q. A. Vu, D. T. Pham, J-H. Lee, S-W. Kim, and Y. H. Lee, *ACS Nano*, 2013, 7, 5940-5947.
24. P. Yang, X. Xiao, Y. Li, Y. Ding, P. Qiang, X. Tan, W. Mai, Z. lin, W. Wu, T. Li, H. Jin, P. Liu, J. Zhou, C. P. Wong, and Z. L. Wang, *ACS Nano*, 2013, 7, 2617-2626.

25. J. Bae, M. K. Song, Y. J. Park, J. M. Kim, M. Liu, and Z. L. Wang, *Angew. Chem. Int. Ed.*, 2011, 50, 1683-1687.
26. K. Wang, Q. Meng, Y. Zhang, Z. Wei, and M. Miao, *Adv. Mater.*, 2013, 25, 1494-1498.
27. J. Tao, N. Liu, W. Ma, L. Ding, L. Li, J. Su, and Y. Gao, *Scientific Reports*, 2013, 3, 1-7.



238x134mm (150 x 150 DPI)